Compositional ordering and quantum transport in $Mo_6S_{9-x}I_x$ nanowires: *Ab initio* calculations

Teng Yang, Savas Berber,* and David Tománek†
Physics and Astronomy Department, Michigan State University, East Lansing, Michigan 48824-2320, USA
(Received 8 February 2008; revised manuscript received 24 March 2008; published 24 April 2008)

We use *ab initio* calculations to study the compositional ordering and quantum transport in $Mo_6S_{9-x}I_x$ nanowires. The skeleton of these nanowires consists of Mo octahedra, which are functionalized by S and I adsorbates and connected by flexible S_3 bridges. The optimum geometries and relative stabilities at different compositions are determined by using density functional theory. We find nanowires with $x=3$ to be particularly stable. Nanowires with other compositions are likely to phase separate into iodine-rich and iodine-depleted domains, some of which should have the $Mo_6S_6I_3$ stoichiometry. Our transport calculations, which are based on the nonequilibrium Green's function formalism, indicate that the nanowires are metallic independent of composition and exhibit a quantum conductance of $G=3G_0$, with the three conductance channels involving the S_3 bridges.

DOI: 10.1103/PhysRevB.77.165426 PACS number(s): 81.05.Zx, 61.46.−w, 68.65.−k, 73.22.−f

I. INTRODUCTION

Combining subnanometer diameter with structural stability and interesting electronic properties, transition metal chalcogenide nanowires have been discussed as a potentially viable alternative to carbon nanotubes[1] for many applications. In particular, $Mo_6S_{9-x}I_x$ nanowires have been extensively studied both experimentally[2–18] and theoretically.[19–21] In contrast to other nanowires and nanotubes, $Mo_6S_{9-x}I_x$ are believed to be metallic independent of their structure[3,19,20] and can be synthesized,[22] dispersed,[5,6] and functionalized[7] in a straightforward manner. Nanomechanical studies indicate a very low shear modulus of the bundled nanowires,[10] suggesting self-lubricating properties and potential applications in nanotribology.[23] Sulfur terminators act as "alligator clips," providing optimum contact to gold leads for molecular electronics applications.

In spite of the numerous studies, several questions about $Mo_6S_{9-x}I_x$ nanowires still await a definitive answer. There is a consensus that the skeleton of these systems consists of Mo octahedra, which are functionalized by S and I adsorbates and connected by bridges containing S or I atoms. Still, there is an open controversy about the atomic arrangement in nanowires with $x=4.5$ and $x=6$, which have been observed as stable compounds. X-ray Diffraction[3] and extended x-ray absorption fine structure[24] studies agree in the identification of Mo octahedra as stable building blocks of the nanowires but disagree about the precise positions of sulfur and iodine. In particular, both iodine[3,24] and sulfur[17,19,20] have been proposed as constituents of the bridges connecting the Mo octahedral building blocks. An additional uncertainty exists, which is whether the connecting bridges contain three[19,25] or four[10,24] atoms.

Obviously, the atomic structure plays a key role in determining the stability and conductance of the nanowires.[26] In spite of the apparent interest in the topic, no conductance data are available that would illustrate the potential of $Mo_6S_{9-x}I_x$ nanowires sandwiched between gold leads for molecular electronics applications. Besides the available structural results for nanowires with $x=4.5$ and $x=6$ stoichiometries, which were assumed to be homogeneous, nothing is known about the structural properties of nanowires with other compositions, which may phase separate into iodine-rich and iodine-depleted domains. Lack of precise structural information also offers a plausible explanation for the apparent discrepancy between the measured and calculated Young's modulus of $Mo_6S_{9-x}I_x$ nanowires[10] with $x=4.5$ and $x=6$.

To address these open points, we combined *ab initio* density functional theory[27,28] and quantum transport calculations based on the nonequilibrium Green's function formalism[29,30] to determine the stability, equilibrium structure, and electronic and transport properties of $Mo_6S_{9-x}I_x$ nanowires in the full composition range. We found the $Mo_6S_6I_3$ nanowire to be particularly stable and identify stoichiometries wherein separation into two phases, one of them being $x=3$, is energetically favorable. Sulfur-terminated wire segments are known to form optimum contacts to gold leads. We find that sulfur forms the most stable bridges connecting the functionalized Mo octahedra and determine the relative stability of bridges containing three or four sulfur atoms. Finally, we determine the conductance of $Mo_6S_{9-x}I_x$ nanowires with $x=3$ and $x=4.5$ sandwiched between two gold leads.

II. THEORY

To determine the optimum geometry, relative stability, and ground-state electronic structure of the nanowires, we used the density functional theory (DFT),[27,28] as implemented in the SIESTA code.[31] We used the Perdew–Zunger[32] form of the exchange-correlation functional in the local density approximation to DFT. The behavior of valence electrons was described by norm-conserving Troullier–Martins pseudopotentials[33] with partial core corrections in the Kleinman–Bylander factorized form.[34] We used a double-zeta basis, including initially unoccupied Mo 5*p* orbitals. We studied the possibility of spin polarization by using the local spin density approximation and found all the nanowires investigated here to be nonmagnetic.

To test the usefulness of these systems as ballistic conductors, we calculated the quantum conductance G of $Mo_6S_{9-x}I_x$ nanowires sandwiched between two Au(111) surfaces as a

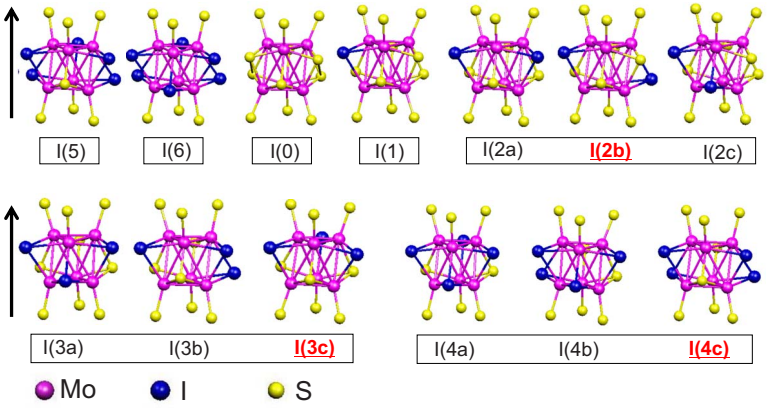

FIG. 1. (Color online) Optimized atomic arrangements within finite building blocks of $Mo_6S_{9-x}I_x$ nanowires. The structures are labeled according to the number of iodine atoms, and structural isomers with the same stoichiometry are distinguished by lowercase Latin characters. The finite clusters have been terminated by S atoms on both sides along the wire direction, which is indicated by the arrows. The most stable isomers for each stoichiometry are underlined and marked in red.

function of the carrier injection energy E. Our calculations were performed by using the nonequilibrium Green's function approach,[29] as implemented in the TRAN-SIESTAC code,[30] and the localized basis set described above.

Our studies focus both on the infinite nanowires and their building blocks, which are depicted in Fig. 1. Infinite nanowires are represented by a periodic arrangement of unit cells with length a containing 30 atoms in 2 formula units of the $Mo_6S_{9-x}I_x$ compound. To describe isolated nanowires while using periodic boundary conditions, we arranged them on a tetragonal lattice with a large interwire separation of 30 Å. We sampled the rather short Brillouin zone of these one dimensional structures by six k points. The charge density and potentials were determined on a real-space grid with a mesh cutoff energy of 150 Ry, which was sufficient to achieve a total energy convergence of better than 2 meV/atom during the self-consistency iterations.

III. RESULTS

A. Optimum functionalization of the building blocks in nanowires

To get a better understanding of the optimum arrangement of iodine and sulfur ligands on the Mo_6 octahedral building blocks in the nanowires, we optimized the structure of all the possible ligand arrangements in $Mo_6S_{12-x}I_x$ systems. To avoid complications caused by stoichiometry-dependent unit cell sizes, we first considered finite nanowire segments. The wire segments were terminated on both sides by sulfur trimers as reference ligands, which act as bridge connectors in the infinite nanowire. Such chalcohalide clusters have been observed in cluster compounds, with a particular oxidation state stabilized by counterions.[35] Even though we consider charge neutral wire segments, the electron count on the Mo_6 octahedra may differ from the infinite nanowire due to the presence of ligands on both sides, causing minor structural and energetic changes. Our results for the equilibrium structure of these finite building blocks with the $0 \leqslant x \leqslant 6$ composition are shown in Fig. 1. For the sake of a fair comparison, we oriented the Mo_6 clusters along the nanowire direction, which is indicated by the arrows, and visually grouped the different structural isomers with the same composition.

Our choice of using sulfur reference ligands is inspired by the results of the combined scanning transmission electron microscopy and x-ray photoelectron spectroscopy study of $Mo_6S_3I_6$ nanowires,[17] suggesting that all bridges connecting Mo_6 octahedra, which are covered by iodine ligands, contain only sulfur atoms.

To interpret our results, we schematically represent the structures of Fig. 1 in Fig. 2. In the representation of Fig. 2, we first lay down the molybdenum octahedra onto one of their faces, which is to be considered the projection plane. Next, we consider the position of ligands decorating all faces except those parallel to the projection plane. Of the six ligands, two triplets will form two equilateral triangles, which are rotated by 180° with respect to each other, in planes parallel to the projection plane. These triangles, with the corners corresponding to the ligand positions, are depicted in Fig. 2. Clearly, structures with $x=0,1,5,6$ iodine atoms have only one structural isomer, which is labeled as I(x) in Figs. 1 and 2. Structures with $x=2,3,4$ iodine atoms have three structural isomers each. Our binding energy results in Fig. 2 suggest that the relative stability of these structural isomers can differ by up to $\approx$0.35 eV. We find that the most stable isomer for each stoichiometry, which is marked by an underlined red label, also has the highest symmetry. Since the interiodine distance is maximized in the favored

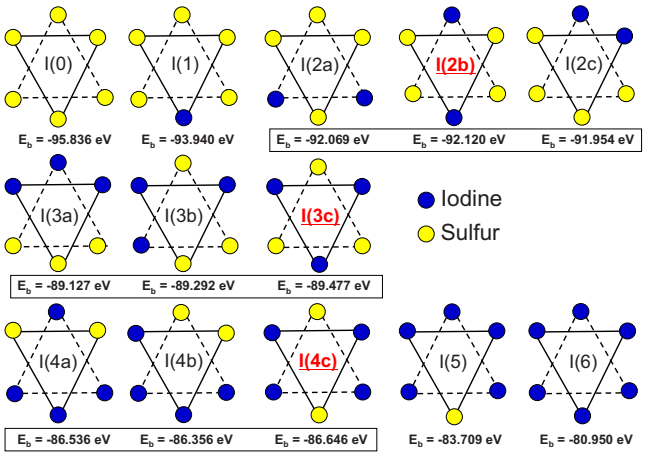

FIG. 2. (Color online) Schematic arrangement of the sulfur and iodine ligand atoms in the structures of Fig. 1, along with the binding energy values E_b with respect to the isolated atoms. The most stable isomers for each stoichiometry are underlined and marked in red.

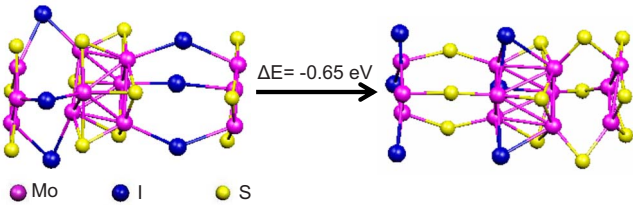

FIG. 3. (Color online) Optimized structure of two isomers with the same $Mo_6S_6I_3$ stoichiometry representing the connection between functionalized Mo_6 building blocks in nanowires by iodine (left) and sulfur (right) bridges.

structures, energy stabilization of the symmetric structures can be understood in terms of reducing Coulomb repulsion.

B. Connection between building blocks in nanowires

In previous studies, both sulfur[17,19,20] and iodine[3,24] have been postulated to form connecting bridges between functionalized Mo_6 building blocks in $Mo_6S_{9-x}I_x$ nanowires. Furthermore, the stability of sulfur- and iodine-based connections has been claimed to be nearly the same.[20] To identify the nature of energetically preferred bridges, we considered two structural isomers of infinite $Mo_6S_6I_3$ nanowires, one with iodine and the other with sulfur bridges connecting the Mo_6-based building blocks. A unit cell of the optimized structures, containing 30 atoms, is shown in Fig. 3. We performed a global structure optimization, including the relaxation of the unit cell size, and found the nanowire connected with sulfur bridges to be energetically more stable by 0.65 eV per 30 atoms, providing further support for the presence of sulfur bridges.

C. Elastic properties of nanowires

In bundles of nanowires, the Young's modulus can be determined from the stress-strain ratio in the wire direction. Experimental observations[10] of high Young's modulus values near 420 GPa in $Mo_{12}S_9I_9$ and $Mo_{12}S_6I_{12}$ suggest that these nanowires should be very rigid in the axial direction. To explain this high rigidity, the bistable S_3 bridges,[19,25] connecting the Mo-based building blocks, were postulated to contain one extra atom in the middle.[10,24] To understand the difference between the S_3 and S_4 bridges in terms of axial rigidity, we determined the stability of $Mo_{12}S_9I_9$ and $Mo_{12}S_{11}I_9$ as a function of the lattice constant. The optimized equilibrium structures and binding energies of these systems are presented in Fig. 4. As seen in Fig. 4(a), owing to the bistability of the two S_3 bridges, the $E(a)$ graph exhibits three minima, the most stable of them corresponding to one short and one long sulfur bridges. In the finite lattice constant range between the different minima, stretching and compression of the nanowire occur at a minimum energy cost. This is no longer true, however, when considering additional compression of a completely compressed or additional stretching of a completely extended nanowire. A quadratic fit of the $E(a)$ plot near the minima, which is depicted by the solid lines in Fig. 4, suggests that there is little difference in the spring constant $k=\partial^2 E/\partial a^2$ of the nanowires represented in

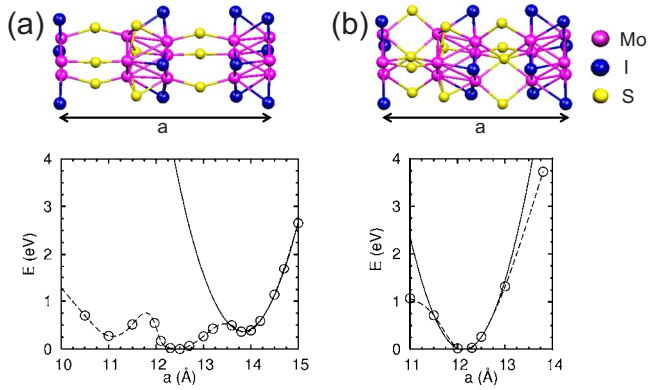

FIG. 4. (Color online) Equilibrium structure and axial rigidity in (a) $Mo_{12}S_9I_9$ and (b) $Mo_{12}S_{11}I_9$ nanowires. The main difference between the compounds is an additional S atom in (b) inserted inside each of the S_3 bridges in (a). E denotes the total energy relative to the optimum structure and a is the lattice constant. The dashed lines are guides to the eye, connecting the data points. Quadratic fits to the data points near the equilibrium, which is related to the axial rigidity, are given by the solid lines.

Figs. 4(a) and 4(b). By using the quadratic fits of Fig. 4, we can calculate the Young's modulus as $Y=k(a_{eq}/A)$, where a_{eq} is the equilibrium lattice constant and A is the cross section of the nanowire. The cross-section area per nanowire in an infinite bundle, where the interwire distance has been optimized[26] to be 9.4 Å, is $A=76.5$ Å^2. This allows us to determine the Young's modulus of $Mo_{12}S_9I_9$ with S_3 bridges as $Y=99$ GPa and that of $Mo_{12}S_{11}I_9$ with S_4 bridges as $Y=109$ GPa. Thus, we conclude that the central atom in the S_4 bridges does not necessarily increase the axial rigidity of the nanowires.

Our results are well within the wide range of reported theoretical and experimental values of the Young's modulus in $Mo_{12}S_xI_y$ nanowires, with calculated data being generally much softer than the observed values.[10,20,36] The calculated value[10] $Y=45$ GPa in $Mo_{12}S_6I_{12}$ nanowires is much smaller than the other reported theoretical values,[20] which are $Y=82$ GPa and $Y=94$ GPa in this system, which contains bistable S_3 bridge connectors, and the $Y=114$ GPa value in $Mo_{12}S_8I_{12}$ nanowires with S_4 bridges.[20] An even larger value $Y=320$ GPa has been predicted for Mo_6S_6 nanowires.[36] By comparing all available data, we conclude that the Young's modulus may sensitively depend on the stoichiometry.

D. Compositional ordering and phase separation in nanowires

Since the synthesis of $Mo_6S_{9-x}I_x$ nanowires occurs in a single-step reaction directly from the elements,[22] we explore the intriguing possibility of forming nanowires with an arbitrary iodine concentration. To account for phase separation, which may be expected in this case, we consider coexistence of domains with different compositions. In the simplest scenario, we consider domains with only two different compositions, which are identified by the iodine concentrations x_1 and x_2. Our objective is to determine the most stable domain structure for $Mo_6S_{9-x}I_x$ nanowires with an arbitrary value of the average iodine concentration $\langle x \rangle$.

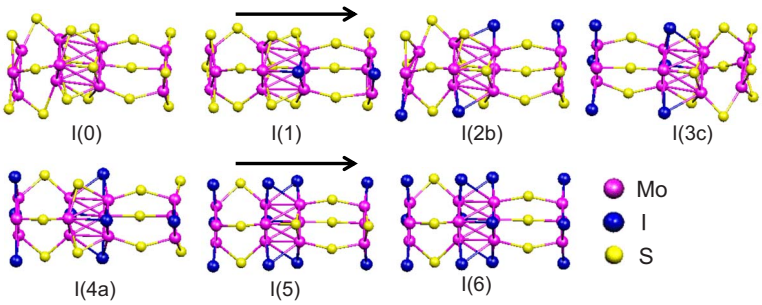

FIG. 5. (Color online) Optimized atomic arrangement within unit cells containing two Mo_6 octahedra in infinitely long $Mo_6S_{9-x}I_x$ nanowires for $0 \leqslant x \leqslant 6$. Only the most stable isomers for each stoichiometry are shown and labeled according to the number of iodine atoms x per formula unit. The nanowire direction is indicated by the arrows.

Before addressing inhomogeneous nanowires, we first identify the most stable structure of homogeneous nanowires. We identified the optimum geometry and binding energy of all nanowires formed with any of the building blocks depicted in Figs. 1 and 2, considering the possibility of parallel and antiparallel alignments of asymmetric building blocks along the nanowire and also the possibility of the bistable sulfur bridges being short or long. As suggested earlier, the most stable structural isomers in the infinite systems, which are depicted in Fig. 5, may deviate from those for the finite building blocks. The binding energy E_b of the most stable structural isomer, which is given per unit cell with respect to isolated atoms, is indicated by the data points in Fig. 6(a). The straight solid line, connecting the data points for structures with no iodine and with no sulfur ligands, represents the expectation value $\langle E_b \rangle$ in case that there is no energy preference for specific ligand arrangements. Similar to alloys,[37] deviations from the straight line for $0 < x < 6$ indicate a tendency to mix or to phase separate.

To better distinguish which structures are more stable than would be expected for a mixture of noninteracting ligands randomly arranged along the nanowire, in Fig. 6(b), we show the energy difference between the optimized uniform systems and the expectation value $\langle E_b \rangle$. The higher-than-average stability of nanowires with $x=3$ suggests the corresponding stoichiometry to be likely present in one of the components in the case of phase separation. On the other hand, we are unlikely to encounter dominant phases with $x=1$ or $x=5$.

Next, we consider a nanowire with the $Mo_6S_{9-\langle x \rangle}I_{\langle x \rangle}$ average composition which separates into two domains. We distinguish the first domain, 1, with the $Mo_6S_{9-x_1}I_{x_1}$ composition and length L_1, from a second domain, 2, with the $Mo_6S_{9-x_2}I_{x_2}$ composition and length L_2. The lengths of the domains are trivially related by $L_1x_1+L_2x_2=(L_1+L_2)\langle x \rangle$. On

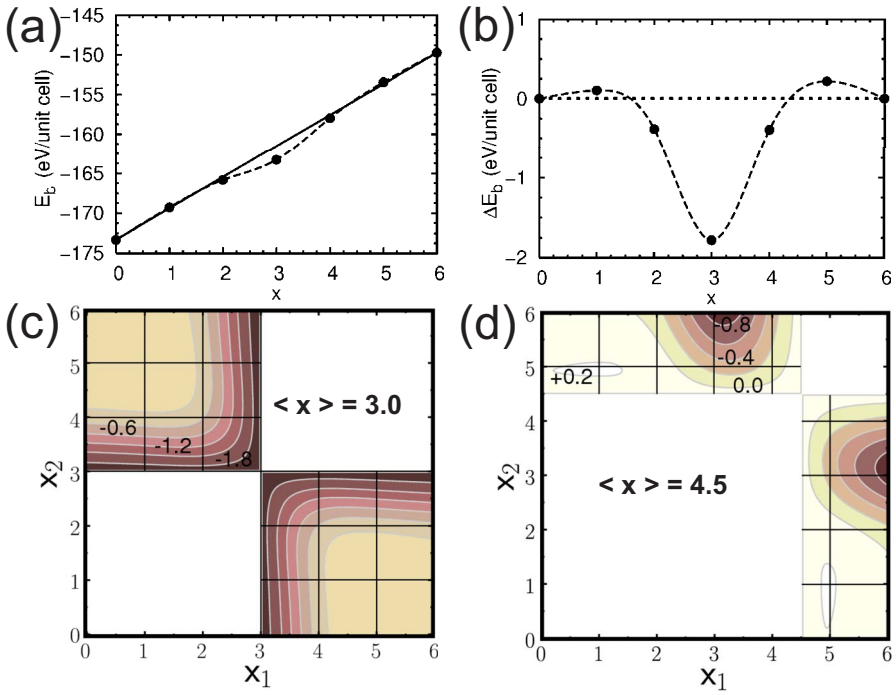

FIG. 6. (Color online) Mixing and phase separation tendency in $Mo_6S_{9-x}I_x$ nanowires. (a) Binding energy E_b as a function of the iodine concentration x. The data points refer to structures depicted in Fig. 5. The solid line, which was obtained by connecting the data points at $x=0$ and $x=6$, depicts the expectation value $\langle E_b \rangle$. The dashed line is a guide to the eye. (b) Energy gain $\Delta E_b(x)$ with respect to $\langle E_b \rangle$. The energy gain associated with phase separation into domains with iodine concentrations x_1 and x_2 is presented in contour plots for systems with $\langle x \rangle = 3.0$ in (c) and $\langle x \rangle = 4.5$ in (d). Quantitative results are only valid for integer values of x_1 and x_2, which are indicated by the grid. The contours in (c) and (d), which are given in units of eV/unit cell, are guides to the eye. The dark areas represent particularly stable stoichiometries.

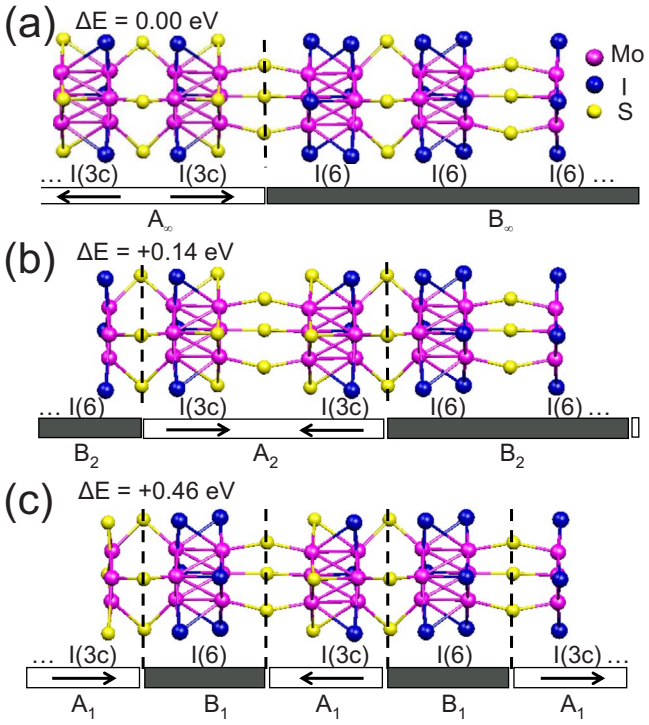

FIG. 7. (Color online) Energy cost associated with grain boundaries in $Mo_6S_{9-x}I_x$ nanowires with $\langle x\rangle=4.5$, consisting of domains A with $x=3$ and domains B with $x=6$. (a) Reference structure, with a single boundary separating domains A and B. (b) A and B domains, containing two Mo_6 octahedra, alternate along the nanowire. (c) A and B domains, each containing a single Mo_6 octahedron, alternate along the nanowire. The energy differences ΔE are given for 2 formula units of $Mo_{12}S_9I_9$, containing 60 atoms.

the other hand, provided that $x_1 \leqslant \langle x\rangle \leqslant x_2$ or $x_2 \leqslant \langle x\rangle \leqslant x_1$, the relative domain lengths are given by $L_1/L=(\langle x\rangle - x_1)/(x_2-x_1)$ and $L_2/L=(x_2-\langle x\rangle)/(x_2-x_1)$ in a nanowire with length $L=L_1+L_2$. Even though both x_1 and x_2 are integers, we find it useful to visualize stability islands by using noninteger values of x_1, x_2 and interpolated energy values presented in Fig. 6(b). The allowable concentration range (x_1,x_2) is shown by shaded areas in Fig. 6(c) for $\langle x\rangle=3.0$ and in Fig. 6(d) for $\langle x\rangle=4.5$. These figures show the contour plot $\Delta E(x_1,x_2)$, corresponding to the energy difference between the expectation value of the binding energy for $\langle x\rangle$ and the weighted average of $E_b(x_1)$ and $E_b(x_2)$. For a given value of $\langle x\rangle$, the pair of integers (x_1,x_2), corresponding to the lowest value of ΔE, identifies the preferred concentrations and relative lengths of the two phases. By inspecting Figs. 6(c) and 6(d) for dark areas, corresponding to particularly stable structures, we find that at least one of the two phases occurs with $x=3$.

In our simple energy estimates underlying Figs. 6(c) and 6(d), we ignored the energy associated with forming domain wall boundaries between regions with different compositions. In Fig. 7, we investigate the energy cost of domain wall boundaries in $Mo_6S_{9-x}I_x$ nanowires with $\langle x\rangle=4.5$, which is addressed in Fig. 6(d). Those results suggest that the nanowire will be most stable when separating into domains A with the $Mo_6S_6I_3$ composition and domains B with the $Mo_6S_3I_6$ composition. To maintain the average stoichiometry, the size of the A and B domains must be equal.

The reference structure of an infinite $Mo_6S_{4.5}I_{4.5}$ nanowire, which is depicted in Fig. 7(a), contains a single domain of phase A, which is separated by a domain wall from a single domain of phase B. As suggested in Figs. 4(a) and 5, the most stable structures of phases A and B, which are labeled A_∞ and B_∞ in Fig. 7(a), exhibit an alternating sequence of short and long sulfur bridges. Figure 4(a) also suggests that in phase A, the orientation of the I(3c) building blocks, which are defined in Fig. 1, should alternate, as indicated by the arrows in Fig. 7(a).

The same $Mo_6S_{4.5}I_{4.5}$ average stoichiometry can be achieved by periodically alternating the A and B domains containing two Mo_6 octahedra, which are labeled A_2 and B_2 in Fig. 7(b). The decrease in stability with respect to the structure of Fig. 7(a), which is reflected in the positive value of the energy cost ΔE, indicates that the creation of additional domain walls is energetically unfavorable. This finding is further supported by an even larger value of ΔE in the structure of Fig. 7(c), where the number of domain walls has doubled with respect to Fig. 7(b). The value of ΔE for the system of Fig. 7(c) is not twice the value for the system of Fig. 7(b) since the local atomic arrangement near the (A_1,B_1) domain boundary differs from that near the (A_2,B_2) domain boundary.

E. Quantum transport in nanowires

One of the most attractive features of $Mo_6S_{9-x}I_x$ nanowires is the presence of S_3 bridges, which are known to form well-defined, stable bonds to Au surfaces. We will calculate quantum conductance in nanowires with the $Mo_6S_{4.5}I_{4.5}$ stoichiometry since $Mo_6S_3I_6$ nanowires do not readily attach to Au electrodes.[38] In the following, we will consider the optimized, frozen structure of infinitely long and of finite nanowires sandwiched between gold leads and determine the quantum conductance of this system within the Landauer–Büttiker formalism.

In the first study, we consider an infinitely long $Mo_6S_{4.5}I_{4.5}$ nanowire, which is shown in Fig. 8(a). We treat one unit cell as the scattering region and define the rest of the nanowire as the semi-infinite leads. The quantum conductance G of the infinite nanowire in units of the conductance quantum G_0 is depicted in Fig. 8(b). The incident energy E of the carriers is with respect to the Fermi level of the leads, which in this case refers to the entire nanowire. $G(E)$ has a nonzero value at $E=0$, suggesting metallic conductivity at very small bias values. Its maximum value of $3G_0$, corresponding to three conduction channels in the nanowire, implies that each atom of the S_3 bridge contributes one conduction channel. The predicted zero conductance value just above $E=0$ suggests that n doping should lead to semiconducting behavior. This explains the observed conductivity drop in nanowires with iodine impurities.[9]

Next, we study the quantum conductance of a finite $Mo_6S_{4.5}I_{4.5}$ nanowire segment sandwiched between Au(111) surfaces as "ideal" leads, which is shown in Fig. 9(a). We selected Au(111) leads since gold forms stable covalent

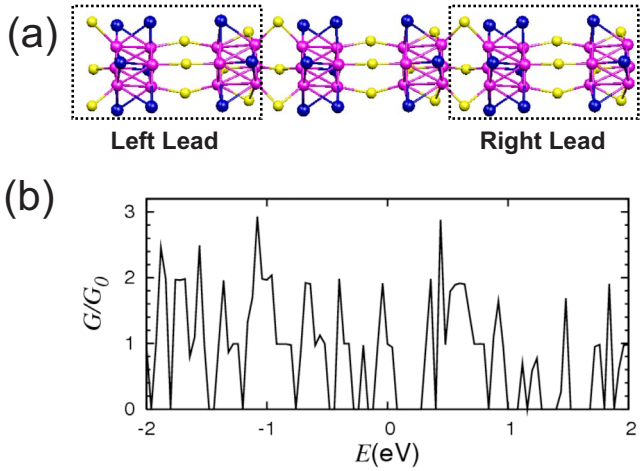

FIG. 8. (Color online) Quantum conductance of an isolated, infinitely long $Mo_6S_{4.5}I_{4.5}$ nanowire. (a) Definition of the scattering and the lead regions in an atomistic model of the nanowire. (b) Quantum conductance G of the nanowire in units of the conductance quantum G_0, which was calculated at zero bias by using a nonequilibrium Green function formalism.

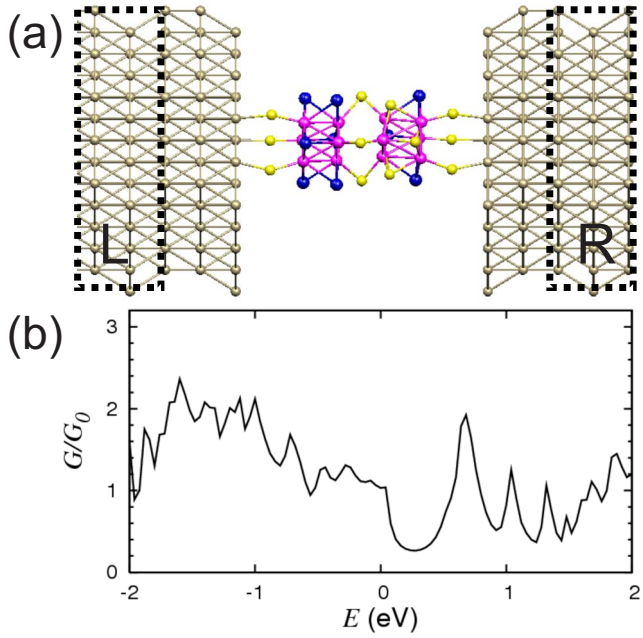

FIG. 9. (Color online) Quantum conductance of an isolated, finite $Mo_6S_{4.5}I_{4.5}$ nanowire sandwiched between Au(111) surfaces. (a) Definition of the scattering and the lead regions in an atomistic model. The left and right leads are semi-infinite gold surfaces, which are indicated by the dashed lines. The scattering region contains the nanowire segment connected to the topmost layers of the Au(111) surface at both sides. (b) Quantum conductance G of the system in units of the conductance quantum G_0, which was calculated at zero bias by using a nonequilibrium Green function formalism.

bonds with sulfur and since the atomic structure at the Au(111) surface is very similar to that of the Mo_6 octahedra. This allows for a well-defined connection between the nanowires and the gold leads by S_3 bridges, causing negligible structural changes near the wire-lead interface. Besides the nanowire segment, we also included the topmost layers of the Au(111) surface at both sides in the scattering region, as indicated in Fig. 9(a), to correctly represent changes in the electronic structure in the contact region. A closer inspection of the charge density of the composite system suggested that changes in the electronic structure are very small, and that including only two to three of the topmost layers of Au(111) in the scattering region should adequately represent the electronic properties and conductance of the system.

The quantum conductance $G(E)$ of the system in units of the conductance quantum G_0 is presented in Fig. 9(b). Here, incident energy E of the carriers is given with respect to the Fermi level of the gold leads. The energy dependence of G suggest a good metallic conductance and closely resembles our results for the infinite nanowire, which is depicted in Fig. 8(b). The reduction from the maximum value $G=3G_0$ in the infinite nanowire, which is caused by the reflection at the nanowire-gold contacts, is relatively small, confirming the high quality of contacts between sulfur-terminated nanostructures and gold. The fact that the dip in the conductance of the infinite nanowire and the sandwiched nanowire segment occurs at the same energy just above $E=0$ suggests that the contact with gold does not significantly change the Fermi level of the nanowire. The filling of the conductance dip above $E=0$ in Fig. 9(b) is caused by the wave functions of the leads, which extend into the nanowire and overlap, thus increasing the conductance of the short nanowire segment.

Our conductance calculations confirm our initial expectation that sulfur atoms form not only stable bridges between functionalized Mo_6 octahedra but also robust and electronically transparent contacts to gold leads. Whereas the conductance of nanowires is generally dominated by contact regions, we find the conductance reduction at the interface between $Mo_6S_{4.5}I_{4.5}$ nanowires and gold to be very small. This is also likely to hold true for other $Mo_6S_{9-x}I_x$ nanowires with a different stoichiometry as long as the Mo-based building blocks are connected by sulfur bridges. Also, the delocalization of conduction electrons within the Mo_6 octahedra should contribute to an excellent electrical conductance behavior of the nanowires[26] independent of the stoichiometry.

IV. SUMMARY AND CONCLUSIONS

We used *ab initio* calculations to study the compositional ordering and quantum transport in $Mo_6S_{9-x}I_x$ nanowires. The skeleton of these nanowires consists of Mo octahedra, which are functionalized by S and I adsorbates and connected by flexible S_3 bridges. The optimum geometries and relative stabilities at different compositions are determined by using density functional theory. We find nanowires with $x=3$ to be particularly stable. Nanowires with other compositions are likely to phase separate into iodine-rich and iodine-depleted domains, some of which should have the $Mo_6S_6I_3$ stoichiometry. Our transport calculations, which are based on the nonequilibrium Green's function formalism, indicate that the nanowires are metallic independent of composition and exhibit a quantum conductance of $G=3G_0$, with the three conductance channels involving the S_3 bridges.

ACKNOWLEDGMENTS

This work was funded by the National Science Foundation under NSF-NSEC Grant No. 425826 and NSF-NIRT Grant No. ECS-0506309. Computational resources have been provided by the Michigan State University High Performance Computing Center.

*Permanent address: Physics Department, Gebze Institute of Technology, 41400 Gebze, Kocaeli, Turkey.
†tomanek@pa.msu.edu

[1] A. Jorio, M. Dresselhaus, and G. Dresselhaus, *Carbon Nanotubes: Advanced Topics in the Synthesis, Structure, Properties and Applications* (Springer, Berlin, 2008).
[2] D. Vrbanic, M. Remskar, A. Jesih, A. Mrzel, P. Umek, M. Ponikvar, B. Jancar, A. Meden, B. Novosel, S. Pejovnik *et al.*, Nanotechnology **15**, 635 (2004).
[3] A. Meden, A. Kodre, J. P. Gomilsek, I. Arcon, I. Vilfan, D. Vrbanic, A. Mrzel, and D. Mihailovic, Nanotechnology **16**, 1578 (2005).
[4] M. Zumer, V. Nemani, B. Zajec, M. Remskar, M. Ploscaru, D. Vengust, A. Mrzel, and D. Mihailovic, Nanotechnology **16**, 1619 (2005).
[5] V. Nicolosi, D. Vrbanic, A. Mrzel, J. McCauley, S. O'Flaherty, C. McGuinness, G. Compagnini, D. Mihailovic, W. J. Blau, and J. N. Coleman, J. Phys. Chem. B **109**, 7124 (2005).
[6] V. Nicolosi, D. Vrbanic, A. Mrzel, J. McCauley, S. O'Flaherty, D. Mihailovic, W. J. Blau, and J. N. Coleman, Chem. Phys. Lett. **401**, 13 (2005).
[7] M. Ploscaru, S. J. Kokalj, M. Uplaznik, D. Vengust, D. Turk, and D. Mihailovic, Phys. Status Solidi B **243**, 3325 (2006).
[8] Z. Kutnjak, D. Vrbanic, S. Pejovnik, and D. Mihailovic, J. Appl. Phys. **99**, 064311 (2006).
[9] B. Bercic, U. Pirnat, P. Kusar, D. Dvorsek, D. Mihailovic, D. Vengust, and B. Podobnik, Appl. Phys. Lett. **88**, 173103 (2006).
[10] A. Kis, G. Csanyi, D. Vrbanic, A. Mrzel, D. Mihailovic, A. Kulik, and L. Forro, Small **3**, 1544 (2007).
[11] D. N. McCarthy, V. Nicolosi, D. Vengust, D. Mihailovic, G. Compagnini, W. J. Blau, and J. N. Coleman, J. Appl. Phys. **101**, 014317 (2007).
[12] J. C. Lasjaunias, A. Sulpice, K. Biljakovic, D. Vengust, and D. Mihailovic, Nanotechnology **18**, 355704 (2007).
[13] D. Vrbanic, S. Pejovnik, D. Mihailovic, and Z. Kutnjak, J. Eur. Ceram. Soc. **27**, 975 (2007).
[14] R. Murphy, V. Nicolosi, Y. Hernandez, D. McCarthy, D. Rickard, D. Vrbanic, A. Mrzel, D. Mihailovic, W. J. Blau, and J. N. Coleman, Scr. Mater. **54**, 417 (2006).
[15] M. I. Ploscaru, S. J. Kokalj, M. Uplaznik, D. Vengust, D. Turk, A. Mrzel, and D. Mihailovic, Nano Lett. **7**, 1445 (2007).
[16] J. J. Doyle, V. Nicolosi, S. M. O'Flaherty, D. Vengust, A. Drury, D. Mihailovic, J. N. Coleman, and W. J. Blau, Chem. Phys. Lett. **435**, 109 (2007).
[17] V. Nicolosi, P. D. Nellist, S. Sanvito, E. C. Cosgriff, S. Krishnamurthy, W. J. Blau, M. L. H. Green, D. Vengust, D. Dvorsek, D. Mihailovic *et al.*, Adv. Mater. (Weinheim, Ger.) **19**, 543 (2007).
[18] V. Nicolosi, D. Vengust, D. Mihailovic, W. J. Blau, and J. N. Coleman, Chem. Phys. Lett. **425**, 89 (2006).
[19] T. Yang, S. Okano, S. Berber, and D. Tomanek, Phys. Rev. Lett. **96**, 125502 (2006).
[20] I. Vilfan and D. Mihailovic, Phys. Rev. B **74**, 235411 (2006).
[21] D. Vengust, F. Pfuner, L. Degiorgi, I. Vilfan, V. Nicolosi, J. N. Coleman, and D. Mihailovic, Phys. Rev. B **76**, 075106 (2007).
[22] A. Jesih, D. Mihailovich, M. Remskar, A. Mrzel, and D. Vrbanic, European Patent No. PCT/EP 2004/001870 (30 June 2005).
[23] L. Joly-Pottuz, F. Dassenoy, J. Martin, D. Vrbanic, A. Mrzel, D. Mihailovic, W. Vogel, and G. Montagnac, Tribol. Lett. **18**, 385 (2005).
[24] G. Paglia, E. S. Bozin, D. Vengust, D. Mihailovic, and S. J. L. Billinge, Chem. Mater. **18**, 100 (2006).
[25] V. Nicolosi, S. Berber, J. N. Coleman, J. Sloan, D. Tománek, D. Mihailovic, and W. J. Blau, presented at the NT'04 Conference on the Science and Application of Nanotubes, San Luis Potosi, Mexico, 19–23 July 2004 (unpublished).
[26] I. Popov, T. Yang, S. Berber, G. Seifert, and D. Tomanek, Phys. Rev. Lett. **99**, 085503 (2007).
[27] P. Hohenberg and W. Kohn, Phys. Rev. **136**, B864 (1964).
[28] W. Kohn and L. Sham, Phys. Rev. **140**, A1133 (1965).
[29] J. Taylor, H. Guo, and J. Wang, Phys. Rev. B **63**, 245407 (2001).
[30] M. Brandbyge, J.-L. Mozos, P. Ordejón, J. Taylor, and K. Stokbro, Phys. Rev. B **65**, 165401 (2002).
[31] J. M. Soler, E. Artacho, J. D. Gale, A. García, J. Junquera, P. Ordejón, and D. Sánchez-Portal, J. Phys.: Condens. Matter **14**, 2745 (2002).
[32] J. P. Perdew and A. Zunger, Phys. Rev. B **23**, 5048 (1981).
[33] N. Troullier and J. L. Martins, Phys. Rev. B **43**, 1993 (1991).
[34] L. Kleinman and D. M. Bylander, Phys. Rev. Lett. **48**, 1425 (1982).
[35] F. A. Cotton and G. Wilkinson, *Advanced Inorganic Chemistry: A comprehensive text* (Interscience, New York, 1966).
[36] I. Vilfan, Eur. Phys. J. B **51**, 277 (2006).
[37] In analogy with the energy gain upon mixing two pure components in an alloy, we define $\Delta E_b = E_b - \langle E_b \rangle$ as the energy gain associated with mixing Mo_6S_9 and $Mo_6S_3I_6$ with S_3 bridges into a homogeneous nanowire with the composition $Mo_6S_{9-\langle x \rangle}I_{\langle x \rangle}$.
[38] D. Mihailovic (private communication).